

**Polarization versus spatial characteristics of optical beams at a planar isotropic interface**

Wojciech Nasalski\*

*Institute of Fundamental Technological Research, Polish Academy of Sciences, Świątokrzyska 21, 00-049 Warsaw, Poland*

(Received 7 July 2006; published 29 November 2006)

Three-dimensional monochromatic optical beams of uniform polarization interacting with a planar boundary between two homogeneous, isotropic, and lossless media are analyzed. Generalized Fresnel transmission and reflection coefficients for beam spectra are given. Interrelations induced by cross-polarization coupling between beam profile and phase and beam polarization, or between spin and orbital angular momentum of beams are derived. Beam transmission for normal incidence is discussed in detail. It is shown that elegant Hermite-Gaussian beams of linear polarization and Laguerre-Gaussian beams of circular polarization, all projected on the interface, are normal modes at this interface. Creation and annihilation of these modes at the interface are shown with total angular momentum being conserved on a single photon level.

DOI: [10.1103/PhysRevE.74.056613](https://doi.org/10.1103/PhysRevE.74.056613)

PACS number(s): 42.25.Gy, 42.60.Jf, 42.25.Ja, 42.50.Xa

**I. INTRODUCTION**

There are two basic families of three-dimensional (3D) solutions of the paraxial wave equation—Hermite-Gaussian (HG) beams of rectangular symmetry and Laguerre-Gaussian (LG) beams of cylindrical symmetry. Both of them form two separate, complete, orthogonal, infinite-dimensional bases for any paraxial beam field with its transverse distribution represented by a square integrated function. In particular, any HG beam can be expressed by a linear combination of LG beams and vice versa [1]. There are also two basic two-dimensional (2D) bases for beam polarization—linear, with transverse magnetic (TM) and transverse electric (TE) states, and circular, with right-handed (CR) and left-handed (CL) states. Any linear state of beam polarization can be represented by a linear combination of circular states and vice versa [2].

Transformations of beam spatial structure and beam polarization are usually implemented optically by astigmatic mode converters and birefringent plates, respectively [3]. Equivalence of their action is similar to the same extent as analogies between orbital angular momentum (OAM), associated with helical phase fronts of beams, and spin angular momentum (SAM), associated with circular polarization of beams [4]. This paper deals with such transformations produced by interaction of 3D beams with planar discontinuity (interface) between two optically transparent semi-infinite media and with interrelations between OAM and SAM that appear as a result of this process.

Spatial profile of the beam intensity and phase of a 3D paraxial beam is independent of beam polarization during propagation in a homogeneous, isotropic, and lossless medium. However, when the beam is incident on a planar discontinuity of medium parameters, its spatial structure and polarization become interrelated. These interrelations result from the action of cross-polarization coupling (XPC) that occurs for incidence of beams of finite cross sections [5]. They cannot be explained only with the help of the standard Fresnel transmission and reflection coefficients, well known

for 2D plane wave incidence. Their generalization to the 3D case appears necessary to deal properly with the beam-interface interactions.

Behavior of beams at medium planar interfaces has been under intense studies for many decades [2,6], and recently, also in the context of several aspects of singular optics [7]. Spatial shifts and deformations of a 3D beam spatial structure have been attracting attention as well [8–10]. This issue, however, remains outside the scope of this contribution. The analysis, although being valid for general incidence of arbitrary beams, will be concentrated mainly on the case of normal incidence of the symmetric HG and LG beams. Such a case can be treated exactly, without the need of resorting to the approximate notions of beam shifts and deformations.

The beams will be considered narrow, with a beam radius of the order of one wavelength at a beam waist. Beam polarization and shape coupling will be defined in a spectral or momentum domain for arbitrary distribution of beam field magnitude, phase, and polarization. In a spatial or direct domain specific cases of the higher-order HG beams of linear TM/TE uniform polarization and LG beams of circular CR/CL uniform polarization will be analyzed in detail. These sets of HG and LG beams will be considered in their biorthogonal versions of complex arguments, known as complex-valued or “elegant” (EHG) and (ELG) beams, respectively [11–13]. Moreover, their commonly known definitions will be further modified by their projection at the interface plane. It appears that such an elegant form of the projected HG and LG transmitted and reflected beam modes is naturally enforced by the interface being illuminated by an arbitrary incident 3D beam. The same process specifies uniquely the coupling between SAM and OAM of circularly polarized ELG beams. These phenomena will be traced here step by step by exact derivation of analytical expressions for the beam field spectral components.

Characteristic features of OAM of LG beams are well known [14]. Let us only mention that, due to the beam symmetry, an average of their transverse momentum is zero and their (mean) OAM, averaged over the total beam field, is intrinsic with respect to their beam axes [15]. On the other hand, the projected ELG beams introduced in this paper are defined with respect to a normal to the interface, not with respect to their beam axes. Therefore, OAM of the projected

\*Electronic address: [wnasal@iptt.gov.pl](mailto:wnasal@iptt.gov.pl)

ELG beams is extrinsic for oblique incidence of beams and intrinsic for their normal incidence. Mainly the latter, intrinsic case of beam incidence is discussed in this paper. Note, however, that contrary to the averaged OAM of LG beams, densities of their OAM depend on position of the axis about which they are measured. That means that OAM density of a LG beam reveals a quasi-intrinsic character of averaged OAM of this beam [16] and that the “intrinsic” and “extrinsic” cases of the beam incidence are interrelated.

Both spin and orbital parts of beam total angular momentum (TAM) attain considerable attention recently due to their possible applications as carriers of information on classical and quantum levels [17–20]. The spin or polarization part can be described in the 2D basis of circular polarization and provides a physical realization of a qubit. The orbital part, usually associated with beam helical wave fronts, has an infinite number of eigenstates and thus may serve as a suitable mean for encoding information in quNits in an  $N$ -dimensional space, with  $N$  restricted only by a finite aperture of an optical system. Both HG and LG beams may be used in these processes as they are interrelated uniquely by HG-LG mode converters [1,3].

Optical coding of information needs sorting beam modes or single photons on the basis on SAM, OAM, and/or TAM. It can be accomplished by interferometric methods capable measuring angular momentum by rotating devices build from prisms, cylindrical lenses, half-wave plates, or other types of phase shifters [21]. It would be interesting to see also application of layered optical structures, composed only of several layers and interfaces, in these processes. This contribution may be regarded as a preliminary step toward such applications. A solution to the problem at hand may appear also useful in analyzing phenomena of transfer of the angular and linear momentum of light beams to a dielectric material [22,23]. Nevertheless, discussion on other, more direct applications, for example, within the range of optical visualization or near-field optics, is out of the scope of this work.

In Sec. II, theoretical analysis of 3D beams in a spectral domain leads to generalization of the standard,  $p$  and  $s$ , Fresnel coefficients. That summarizes results derived by the author in the past in another context [5,24,25] still given for arbitrary beam profile, phase, and polarization. In Sec. III, decomposition of beam transmission and reflection into parts characteristic to normal and critical incidence of total internal reflection (TIR) will be presented, together with distinct properties of their transmission and reflection partial coefficients. Beam field redistribution between opposite orthogonal polarization TM and TE or CR and CL components will be exactly derived in a spectral domain.

Transmission of the projected elegant higher-order HG and LG beams of uniform polarization, incident at normal incidence upon the interface will be analyzed in a spatial domain in Sec. IV. Theoretical results will be illuminated by numerical simulations. The beam mode conversion through the XPC effect at the interface will be described in detail. Definitions of beam normal modes at the interface will be given. Coupling between OAM and SAM of beams at the interface will be explained in Sec. V in terms of a conservation principle of their TAM. It will be shown that the analysis

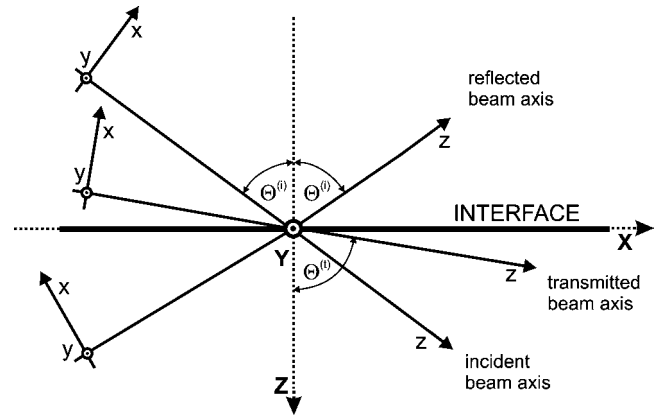


FIG. 1. Interface  $OXYZ$  and beam  $Oxyz$  reference frames for transmission and reflection viewed in a beam plane of incidence  $X-Z$ ; local frames  $Ox_p y_s z_k$  are given by rotation of the plane  $X-Z$  by an azimuthal angle  $\varphi$  around the axis  $Z$ . Beam waists are placed in centers of beam frames, incidence of internal reflection is assumed.

accounts this principle on both macroscopic and single photon levels. Conclusions close the paper in Sec. VI.

## II. ACTION OF THE INTERFACE IN A SPECTRAL DOMAIN

Spectral components of 3D beams at the interface are defined in three local reference frames  $Ox_p y_s z_k$ , each one for the incident ( $b=i$ ), reflected ( $b=r$ ), and transmitted ( $b=t$ ) beams [5]. These three frames are defined for separate spectral (plane-wave) components of the beams. The total field of the beams is defined in frames  $Oxyz$ , one frame for each beam. There is also an interface frame  $OXYZ$ , for the total field of all three beams at the interface, here placed at the plane  $Z=0$ . The  $z_k$  axes indicate propagation directions of the plane waves, the  $z$  axes coincide with the propagation directions of the beams, and the  $Z$  axis is normal to the interface. Geometry of the problem is outlined in Fig. 1.

The plane  $x_p-z_k$  is the local incidence plane and the planes  $x-z$  or  $X-Z$  define the beam or main incidence plane [5]. There are also three transverse planes: the local transverse plane  $x_p-y_s$ , for one spectral beam field component, the beam transverse plane  $x-y$ , for the total beam field, and the interface plane  $X-Y$ , transverse to the normal  $\hat{e}_Z$  to the interface. For normal incidence the beam transverse plane  $x-y$  coincides with the interface plane  $X-Y$ . For oblique incidence the  $z$ -axis makes with the  $Z$  axis an incidence angle  $\theta^{(i)}$  of the incident beam.

In the local reference frames  $Ox_p y_s z_k$ , one transverse spectral component  $\tilde{E}^{(b)}$  of the beam field is given by the scalar multiplication  $\hat{e}_{(p,s)} \tilde{E}_{(p,s)}^{(b)}$  of beam polarization  $\hat{e}_{(p,s)} = [\hat{e}_p, \hat{e}_s]$  and field amplitude  $\tilde{E}_{(p,s)}^{(b)} = [\tilde{E}_p^{(b)}, \tilde{E}_s^{(b)}]^T$  vectors;  $T$  means transpose. The amplitude vector is composed of  $p$  and  $s$  field components  $\tilde{E}_p^{(b)}$  and  $\tilde{E}_s^{(b)}$  in the local transverse plane  $x_p-y_s$ . A pair of the unit vectors— $\hat{e}_p$  placed in this plane and  $\hat{e}_s$  orthogonal to this plane—spans the local 2D polarization

space transverse to the wave vector  $\underline{k}^{(b)} = [k_\perp, k_Z^{(b)}]$  of one spectral field component [5].

The Fresnel transmission and reflection coefficients, generalized to the case of beams with finite cross sections, have been exactly derived in the beam frames  $Oxyz$  [25]. However, the beam-interface interactions are more conveniently described in the interface reference frame  $OXYZ$  [24]. In this frame, the transverse  $k_\perp$ ;  $k_\perp^2 = k_X^2 + k_Y^2$ , and longitudinal  $k_Z^{(b)}$ ;  $(k_Z^{(b)})^2 = (k^{(b)})^2 - k_\perp^2$ , components of  $\underline{k}^{(b)}$  determine, through  $k_\perp = k^{(b)} \sin \vartheta^{(b)}$ ,  $k_X = k_\perp \cos \varphi$  and  $k_Y = k_\perp \sin \varphi$ , the polar  $\vartheta^{(b)}$  and azimuthal  $\varphi$  incidence angles in the local cylindrical coordinate frame  $Ok_\perp \varphi k_Z^{(b)}$ . For  $\varphi=0$  and  $\vartheta^{(i)} = \theta^{(i)}$ , the local plane  $x_p - z_k$  coincides with the beam incidence plane  $x - z$ . For brevity, dependence of the field vectors  $\underline{\tilde{E}}^{(b)}$  and  $\underline{\tilde{E}}^{(b)}_{(p,s)}$  on  $k_X$ ,  $k_Y$ , and  $Z$  are taken through the paper as implicit.

### A. Beam transmission

For each spectral transverse components  $\underline{\tilde{E}}^{(b)}$  of the incident ( $b=i$ ) and transmitted ( $b=t$ ) beam fields,

$$\underline{\tilde{E}}^{(b)} = \underline{\tilde{E}}_p^{(b)} \hat{e}_p + \underline{\tilde{E}}_s^{(b)} \hat{e}_s, \quad (1)$$

$$\underline{\tilde{E}}^{(t)}_{(p,s)} = \underline{t}_{(p,s)} \underline{\tilde{E}}^{(i)}_{(p,s)}, \quad (2)$$

the field vector amplitudes  $\underline{\tilde{E}}^{(b)}_{(p,s)}$  are composed of the transverse field components  $\underline{\tilde{E}}_p^{(b)}$  and  $\underline{\tilde{E}}_s^{(b)}$ . The elements of the diagonal transmission matrix  $\underline{t}_{(p,s)}$  are the well-known Fresnel coefficients  $t_p \equiv t_p(\vartheta^{(i)})$  and  $t_s \equiv t_s(\vartheta^{(i)})$ , which already account for the Snell law. The total field of the beam is composed of continuum of plane waves defined in different local incidence planes  $x_p - z_k$ . However, all spectral components of the beam field need to be presented in one reference frame, usually taken as the beam frame  $Oxyz$  [26]. Here, the interface frame  $OXYZ$  is chosen instead. In this frame, the definitions (1) and (2) should read

$$\underline{\tilde{E}}^{(b)} = \underline{\tilde{E}}_X^{(b)} \hat{e}_X + \underline{\tilde{E}}_Y^{(b)} \hat{e}_Y, \quad (3)$$

$$\underline{\tilde{E}}^{(t)}_{(X,Y)} = \underline{t}_{(X,Y)} \underline{\tilde{E}}^{(i)}_{(X,Y)}, \quad (4)$$

with new polarization vector  $\hat{e}_{(X,Y)} = [\hat{e}_X, \hat{e}_Y]$ , amplitude vector  $\underline{\tilde{E}}_{(X,Y)} = [\underline{\tilde{E}}_X^{(b)}, \underline{\tilde{E}}_Y^{(b)}]^T$ , and transmission matrix  $\underline{t}_{(X,Y)}$ .

Further analysis aims to find field amplitudes and transmission coefficients for each spectral field component in the frame  $OXYZ$  by conversion of the expressions (1) and (2), given in any local incidence plane  $\varphi \neq 0$ , to their counterparts (3) and (4) in the global incidence plane. It can be accomplished by two 3D rotations:  $\underline{R}_Y$  about the  $Y$  axis by  $\vartheta^{(b)}$  and  $\underline{R}_Z$  about the  $Z$  axis by  $\varphi$  or by projection of  $\underline{\tilde{E}}^{(b)}_{(p,s)}$  on the plane  $X-Z$  [5,24]. However, after taking into account the divergence equation  $\underline{\tilde{E}}_Z^{(b)} k_Z^{(b)} = -\underline{\tilde{E}}_{(X,Y)} \circ \underline{k}_\perp$ , only the 2D rotation matrices,

$$\underline{R}_Y(\vartheta^{(b)}) = (k^{(b)})^{-1} \begin{bmatrix} k_Z^{(b)} & 0 \\ 0 & k^{(b)} \end{bmatrix} = \begin{bmatrix} \cos \vartheta^{(b)} & 0 \\ 0 & 1 \end{bmatrix}, \quad (5)$$

$$\underline{R}_Z(\varphi) = k_\perp^{-1} \begin{bmatrix} k_X & -k_Y \\ k_Y & k_X \end{bmatrix} = \begin{bmatrix} \cos \varphi & -\sin \varphi \\ \sin \varphi & \cos \varphi \end{bmatrix}, \quad (6)$$

may be used instead in evaluation of the field components and transmission matrix elements,

$$\underline{\tilde{E}}^{(b)}_{(X,Y)} = \underline{R}_Z(\varphi) \underline{R}_Y(\vartheta^{(b)}) \underline{\tilde{E}}^{(b)}_{(p,s)}, \quad (7)$$

$$\underline{t}_{(X,Y)} = \underline{R}_Z(\varphi) \underline{R}_Y(\vartheta^{(t)}) \underline{t}_{(p,s)} \underline{R}_Y^{-1}(\vartheta^{(i)}) \underline{R}_Z^{-1}(\varphi). \quad (8)$$

That yields

$$\begin{bmatrix} \underline{\tilde{E}}_X^{(b)} \\ \underline{\tilde{E}}_Y^{(b)} \end{bmatrix} = (k^{(b)} k_\perp)^{-1} \begin{bmatrix} k_X k_Z^{(b)} & -k_Y k^{(b)} \\ k_Y k_Z^{(b)} & k_X k^{(b)} \end{bmatrix} \begin{bmatrix} \underline{\tilde{E}}_p^{(b)} \\ \underline{\tilde{E}}_s^{(b)} \end{bmatrix}, \quad (9)$$

$$\underline{t}_{(X,Y)} = k_\perp^{-2} \begin{bmatrix} \eta t_p k_X^2 + t_s k_Y^2 & (\eta t_p - t_s) k_X k_Y \\ (\eta t_p - t_s) k_X k_Y & \eta t_p k_Y^2 + t_s k_X^2 \end{bmatrix}, \quad (10)$$

where  $\eta = \cos \vartheta^{(t)} / \cos \vartheta^{(i)}$ . Still, by introduction of the linear polarization parameter in the spectral domain of the incident beam

$$\tilde{\chi}_{(X,Y)}^{(b)} = \frac{\underline{\tilde{E}}_X^{(b)}}{\underline{\tilde{E}}_Y^{(b)}}, \quad (11)$$

$b=i$ , the transmission matrix  $\underline{t}_{(X,Y)}$  can be rewritten into the diagonal form [24]:

$$\underline{t}_{(X,Y)} = \begin{bmatrix} \eta t_{TM} & 0 \\ 0 & t_{TE} \end{bmatrix} = \begin{bmatrix} \eta t_p + \Delta_{TM} & 0 \\ 0 & t_s + \Delta_{TE} \end{bmatrix}, \quad (12)$$

$$\Delta_a \equiv \Delta_a(\vartheta^{(i)}, \varphi) = (\eta t_p - t_s) k_\perp^{-2} k_Y [(\tilde{\chi}_{(X,Y)}^{(i)})^{\mp 1} k_X \mp k_Y], \quad (13)$$

where  $a=TM$  ( $a=TE$ ) for the upper (lower) signs in (13). In the following, the parameter  $\tilde{\chi}_{(X,Y)}^{(i)}$  will be assumed as independent of  $k_X$  and  $k_Y$ , that it remains common for all points of the interface plane. That means that the incident beam is considered in an arbitrary uniform polarization state.

The coefficients  $t_{TM} \equiv t_{TM}(\vartheta^{(i)}, \varphi; \tilde{\chi}_{(X,Y)}^{(i)})$  and  $t_{TE} \equiv t_{TE}(\vartheta^{(i)}, \varphi; \tilde{\chi}_{(X,Y)}^{(i)})$  of transmission should be understood as the Fresnel coefficients  $\eta t_p$  and  $t_s$  modified, due to the 3D character of the beams, by the modification terms  $\Delta_{TM}$  and  $\Delta_{TE}$ , respectively, both proportional to the difference  $\eta t_p - t_s$  of these coefficients. They consist of the first-order and the second-order ingredients with respect to  $k_Y$  and disappear at the beam incidence plane, i.e., for  $k_Y=0$ . For pure  $TM$  and  $TE$  incident polarization ( $\tilde{\chi}_{(X,Y)}^{(i)} = 0$  and  $\tilde{\chi}_{(X,Y)}^{(i)} = \infty$ , respectively), and the coefficients  $\eta t_p$  and  $t_s$  are modified only by the second-order terms  $\mp (\eta t_p - t_s) k_Y^2 k_\perp^{-2}$  [24].

### B. Beam reflection

Similar considerations to those given in Sec. II can be repeated for the reflected beam (cf. Fig. 1). The transverse field spectral components

$$\tilde{\underline{E}}^{(r)} = \tilde{E}_p^{(r)} \hat{e}_p + \tilde{E}_s^{(r)} \hat{e}_s \quad (14)$$

are defined in the local frame  $Ox_p y_s z_k$  by the field amplitude  $\tilde{\underline{E}}_{(p,s)}^{(r)} = [\tilde{E}_p^{(r)}, \tilde{E}_s^{(r)}]^T$  and polarization  $\hat{e}_{(p,s)}$  vectors. The new amplitude  $\tilde{\underline{E}}_{(-X,Y)}^{(r)}$  and polarization  $\hat{e}_{(-X,Y)}$  vectors, defined in the interface  $OXYZ$  frame, can be obtained by the rotation (5) and (6) and inversion  $\underline{R}_Y$ ;  $-\underline{R}_{I,XX} = 1 = \underline{R}_{I,YY}$ , transformations applied to  $\tilde{\underline{E}}_{(p,s)}^{(r)}$  and  $\hat{e}_{(p,s)}$  in the appropriate order, or equivalently, by projection of  $\tilde{\underline{E}}_{(p,s)}^{(r)}$  on the plane  $X-Z$  [5,24],

$$\tilde{\underline{E}}_{(-X,Y)}^{(r)} = \underline{R}_Y \underline{R}_Z(\varphi) \underline{R}_Y(\vartheta^{(r)}) \underline{R}_Y \tilde{\underline{E}}_{(p,s)}^{(r)}, \quad (15)$$

$$\begin{bmatrix} -\tilde{E}_X^{(r)} \\ \tilde{E}_Y^{(r)} \end{bmatrix} = (k^{(r)} k_\perp)^{-1} \begin{bmatrix} k_X k_Z^{(r)} & k_Y k^{(r)} \\ -k_Y k_Z^{(r)} & k_X k^{(r)} \end{bmatrix} \begin{bmatrix} \tilde{E}_p^{(r)} \\ \tilde{E}_s^{(r)} \end{bmatrix}. \quad (16)$$

The reflection matrix  $\underline{r}_{(-X,Y)}$  can be then evaluated from the local or Fresnel reflection matrix  $\underline{r}_{(p,s)}$ , with its diagonal elements  $r_p \equiv r_p(\vartheta^{(i)})$  and  $r_s \equiv r_s(\vartheta^{(i)})$ , by the application the inversion and rotation matrices in appropriate order, what yields the definition the reflection matrix in the frame  $\hat{e}_{(-X,Y)}$  [5],

$$\underline{r}_{(-X,Y)} = \underline{R}_Y \underline{R}_Z(\varphi) \underline{R}_Y(\vartheta^{(r)}) \underline{R}_Y \underline{r}_{(p,s)} \underline{R}_Y^{-1}(\vartheta^{(i)}) \underline{R}_Z^{-1}(\varphi), \quad (17)$$

$$\underline{r}_{(-X,Y)} = k_\perp^{-2} \begin{bmatrix} r_p k_X^2 - r_s k_Y^2 & (r_p + r_s) k_X k_Y \\ -(r_p + r_s) k_X k_Y & -r_p k_Y^2 + r_s k_X^2 \end{bmatrix}, \quad (18)$$

where  $\tilde{\underline{E}}_{(-X,Y)}^{(r)} = \underline{r}_{(-X,Y)} \tilde{\underline{E}}_{(X,Y)}^{(i)}$ .

Next, introduction of the polarization parameter  $\tilde{\chi}_{(X,Y)}^{(i)}$  makes  $\underline{r}_{(-X,Y)}$  diagonal [24]

$$\underline{r}_{(-X,Y)} = \begin{bmatrix} r_{TM} & 0 \\ 0 & r_{TE} \end{bmatrix} = \begin{bmatrix} r_p - \Delta_{TM} & 0 \\ 0 & r_s + \Delta_{TE} \end{bmatrix}, \quad (19)$$

where  $r_{TM} \equiv r_{TM}(\vartheta^{(i)}, \varphi; \tilde{\chi}_{(X,Y)}^{(i)})$  and  $r_{TE} \equiv r_{TE}(\vartheta^{(i)}, \varphi; \tilde{\chi}_{(X,Y)}^{(i)})$  mean the Fresnel coefficients  $r_p$  and  $r_s$  modified by the terms  $\Delta_{TM}$  and  $\Delta_{TE}$  (12) and (13), both proportional to the sum  $r_p + r_s$  of these coefficients. Equation (12) for transmission and (19) for reflection, together with the definition (13) of the beam spectra modifications, explicitly show differences between the 3D beam and 2D beam cases. The terms  $\Delta_{TM}$  and  $\Delta_{TE}$  disappear for plane waves and 2D beams. Such effects as XPC, interrelations between beam spin and orbital angular momentum, transverse modifications of beam profile, phase, and polarization are specific only to the 3D case.

Note that the transmission (12) and reflection (19) matrices are exact for any plane wave of which the incident beam is composed. They are dependent on each other and interrelated through the continuity of the field components tangent to the interface [24]

$$1 - r_p = \eta t_p, \quad 1 + r_s = t_s, \quad (20)$$

$$1 - r_{TM} = \eta t_{TM}, \quad 1 + r_{TE} = t_{TE}. \quad (21)$$

Equation (21) is given in the main plane of incidence, that is for  $\varphi=0$ , and Eq. (20) is given in the local plane of incidence, that is, in general, for  $\varphi \neq 0$ .

### III. NORMAL VERSUS CRITICAL INCIDENCE OF BEAMS

The Fresnel coefficients defined for plane waves are interrelated through the field continuity relations (20) at the interface or equivalently by

$$\frac{1}{2}(\eta t_p + t_s) = 1 - \frac{1}{2}(r_p - r_s), \quad (22)$$

$$\frac{1}{2}(\eta t_p - t_s) = -\frac{1}{2}(r_p + r_s). \quad (23)$$

For normal incidence Eqs. (22) and (23) read  $\eta t_p = t_s = 1 - r_p = 1 + r_s$  and  $0=0$ , respectively. Moreover, they read  $1=1$  for critical incidence of TIR. That suggests that Eq. (22) can be associated with normal incidence and Eq. (23) with critical incidence of one separate spectral component of the beams. This form of the field continuity relations leads to a special type of beam field decomposition, particularly suitable in treatment of beams at the interface.

#### A. Field decomposition in the linear polarization basis

The transmission (12) and reflection (19) matrices can be decomposed in such a way that the separate terms of the relations (22) and (23) stand for the amplitudes of separate parts of the decomposition of these matrices. In the TM/TE polarization basis  $\hat{e}_{(X,Y)}$ , this decomposition takes the following form:

$$\underline{t}_{(X,Y)} = +\frac{1}{2}(\eta t_p + t_s) \begin{bmatrix} 1 & 0 \\ 0 & 1 \end{bmatrix} + \frac{1}{2}(\eta t_p - t_s) k_\perp^{-2} \begin{bmatrix} k_X^2 - k_Y^2 & 2k_X k_Y \\ 2k_X k_Y & -k_X^2 + k_Y^2 \end{bmatrix}, \quad (24)$$

$$\underline{r}_{(-X,Y)} = -\frac{1}{2}(r_p - r_s) \begin{bmatrix} -1 & 0 \\ 0 & 1 \end{bmatrix} + \frac{1}{2}(r_p + r_s) k_\perp^{-2} \begin{bmatrix} k_X^2 - k_Y^2 & 2k_X k_Y \\ -2k_X k_Y & k_X^2 - k_Y^2 \end{bmatrix}, \quad (25)$$

now explicitly dependent on the azimuthal angle  $\varphi$  through the relations  $k_X^2 - k_Y^2 = k_\perp^2 \cos 2\varphi$  and  $2k_X k_Y = k_\perp^2 \sin 2\varphi$ . The matrix decomposition (24) and (25), together with a  $Z$  component of the field

$$\tilde{E}_Z^{(b)} = -\frac{\tilde{E}_X^{(b)} k_X + \tilde{E}_Y^{(b)} k_Y}{k_Z^{(b)}} \quad (26)$$

describe explicitly characteristic properties of beam transmission and reflection. They depend on the beam incidence angle, polarization and transverse field structure, and on the

type of media of which the interface is composed.

The diagonal part of the transmission (24) matrix is proportional to the identity matrix. Therefore, it does not change the polarization state of the beam and remains common for any polarization base used in the beam field representation. The same concerns, up to the sign changes, the reflection matrix (25). For critical incidence of TIR, the amplitudes of the diagonal ingredients amount  $\frac{1}{2}(\eta_p + t_s) = 1$  and  $\frac{1}{2}(r_p - r_s) = 0$ , respectively; that is, they describe total transmission of the beams. On the contrary, the amplitudes of the second, XPC parts of the matrices (24) and (25) yield  $\frac{1}{2}(\eta_p - t_s) = -1$  and  $\frac{1}{2}(r_p + r_s) = 1$  for critical incidence of TIR. For normal incidence, both of them equal zero. Therefore, the first parts in Eqs. (24) and (25) can be associated with normal incidence and the second, with critical incidence of TIR. For incidence other than normal and critical, all amplitudes in the decompositions in (24) and (25) take nonzero values.

### B. Field decomposition in the circular polarization basis

In the circular polarization frame  $\hat{e}_{(R,L)} = [\hat{e}_R, \hat{e}_L]$ , composed of CR and CL polarization vectors  $\hat{e}_R$  and  $\hat{e}_L$ , respectively, the basis  $\hat{e}_{(R,L)}$  and the field amplitudes  $\tilde{E}_{(R,L)}^{(b)} = [\tilde{E}_R^{(b)}, \tilde{E}_L^{(b)}]^T$  in this basis are obtained from the linear basis  $\hat{e}_{(X,Y)}$  and the field amplitudes  $\underline{E}_{(\pm X,Y)}^{(b)}$  by the unitary transformation  $\underline{U}$ ;  $U_{RX} = 2^{-1/2} = U_{LY}$  and  $-U_{RY} = i2^{-1/2} = U_{LX}$ , that is by  $\hat{e}_{(R,L)} = \hat{e}_{(X,Y)} \underline{U}^+$  and  $\tilde{E}_{(R,L)}^{(b)} = \underline{U} \underline{E}_{(\pm X,Y)}^{(b)}$  (the superscripted plus sign means Hermitian conjugate). This yields

$$\tilde{E}^{(b)} = \tilde{E}_R^{(b)} \hat{e}_R + \tilde{E}_L^{(b)} \hat{e}_L, \quad (27)$$

$$\hat{e}_{(R,L)} = 2^{-1/2} [\hat{e}_X + i\hat{e}_Y, \hat{e}_X - i\hat{e}_Y], \quad (28)$$

with transverse and longitudinal field components expressed by

$$\tilde{E}_{(R,L)}^{(t)} = 2^{-1/2} [\tilde{E}_X^{(t)} - i\tilde{E}_Y^{(t)}, \tilde{E}_X^{(t)} + i\tilde{E}_Y^{(t)}]^T, \quad (29)$$

$$\tilde{E}_{(R,L)}^{(r)} = 2^{-1/2} [-\tilde{E}_X^{(r)} - i\tilde{E}_Y^{(r)}, -\tilde{E}_X^{(r)} + i\tilde{E}_Y^{(r)}]^T, \quad (30)$$

$$\tilde{E}_Z^{(b)} = \mp 2^{-1/2} [\tilde{E}_R^{(b)} \exp(\pm i\varphi) + \tilde{E}_L^{(b)} \exp(\mp i\varphi)] \tan \vartheta^{(b)}. \quad (31)$$

The upper (lower) signs in (31) pertain the transmitted ( $b=t$ ) (reflected;  $b=r$ ) beam. Note that  $\exp(\pm i\varphi) = (k_X \pm ik_Y) k_\perp^{-1}$  and  $\tan \vartheta^{(b)} = k_\perp (k_Z^{(b)})^{-1}$ . The winding number of the Z components of all beams—incident, transmitted, and reflected—is larger (lower) by 1 than that of the transverse field component of the CR (CL) polarization. The transmission  $\underline{t}_{(R,L)} = \underline{U} \underline{t}_{(X,Y)} \underline{U}^+$  and reflection  $\underline{r}_{(R,L)} = \underline{U} \underline{r}_{(-X,Y)} \underline{U}^+$  matrices

$$\underline{t}_{(R,L)} = \frac{1}{2}(\eta_p + t_s) \begin{bmatrix} 1 & 0 \\ 0 & 1 \end{bmatrix} + \frac{1}{2}(\eta_p - t_s) \times \begin{bmatrix} 0 & \exp(-2i\varphi) \\ \exp(+2i\varphi) & 0 \end{bmatrix}, \quad (32)$$

$$\underline{r}_{(R,L)} = \frac{1}{2}(r_p - r_s) \begin{bmatrix} 0 & 1 \\ 1 & 0 \end{bmatrix} + \frac{1}{2}(r_p + r_s) \times \begin{bmatrix} \exp(+2i\varphi) & 0 \\ 0 & \exp(-2i\varphi) \end{bmatrix}, \quad (33)$$

can be then decomposed into two parts: diagonal and anti-diagonal, with distinct polarization properties.

The diagonal part of the transmission matrix  $\underline{t}_{(R,L)}$  does not change the beam polarization. It modifies only amplitudes of beam spectral components by the factor  $\frac{1}{2}(\eta_p + t_s)$ . The anti-diagonal part of  $\underline{t}_{(R,L)}$ , with its amplitude  $\frac{1}{2}(\eta_p - t_s)$ , represents the pure XPC effect of the beam-interface interaction; the CR polarization of the incident beam is replaced by the CL polarization under beam transmission and vice versa. Moreover, this part of the transmission matrix changes, in the beam center, a topological charge of the beam by two. For the incident CR (CL) polarization the topological charge is increased (decreased) by two in the CL (CR) polarization of the transmitted beam.

For the beam reflection, due to the inversion  $\underline{R}_Z$ , the diagonal and anti-diagonal components of the reflection matrix are replaced with respect to their roles in the beam transmission. The first part of  $\underline{r}_{(R,L)}$ , this with the amplitude  $\frac{1}{2}(r_p - r_s)$ , changes the beam polarization state to the opposite one, but without changes in the beam topological charge. On the contrary, the second part of  $\underline{r}_{(R,L)}$ , this with the amplitude  $\frac{1}{2}(r_p + r_s)$ , does not change the beam polarization. Instead, due to the XPC effect at the interface, it increases (decreases) the topological charge of the reflected beam by two for the CR (CL) polarization of the incident beam.

The transmission  $\underline{t}_{(R,L)}$  (32) and reflection  $\underline{r}_{(R,L)}$  (33) matrices in the circular CR/CL basis are equivalent to their counterparts  $\underline{t}_{(X,Y)}$  (24) and  $\underline{r}_{(-X,Y)}$  (25) in the linear TM/TE basis. All of them describe completely, in the spectral domain, the transmission and reflection phenomena of 3D beams of arbitrary shape and polarization incident upon the interface at an arbitrary incidence angle.

### IV. ACTION OF THE INTERFACE IN A SPATIAL DOMAIN

Consider now characteristic features of the beam-interface interactions in the spatial domain. 3D beams of finite cross sections are usually expressed by their spectral representation, which in the reference frame  $OXYZ$  yields

$$\underline{E}^{(b)}(X, Y, Z) = \left(\frac{w_w}{2\pi}\right)^2 \exp(\pm ik^{(b)}_z Z) \int dk_X \int dk_Y \tilde{E}^{(b)} \times (k_X, k_Y, Z) \exp[i(k_X X + k_Y Y)], \quad (34)$$

where harmonic dependence on time  $\exp(-i\omega t)$  is assumed and suppressed. Note that, although the representation (34) is exact, for clarity of further considerations the beam vector amplitudes  $\tilde{E}^{(b)}$  are now defined as dependent on Z, the convention typical for paraxial beams [27]. In this way, the representation (34) is valid for paraxial and nonparaxial beams, provided that in the second choice the paraxial beam profile and phase distribution are imposed only at one transverse

plane, for instance, as taken below, at the interface plane  $Z=0$ .

The representation (34) translates characteristic features of beams from the spectral domain to the spatial domain. In general, the integration can be accomplished only numerically. Sometimes, however, for some specific incident beam distributions, it can be obtained also directly by analytical evaluation of the beam fields in some specific polarization basis. For HG or LG beams of arbitrary order, this evaluation is possible under fulfilment of some additional conditions, evident from further considerations.

The analysis will be restricted only to a single interface. However, due to the diagonal form of matrices (12) and (19), the results can be directly generalized to the case of beams at isotropic layered structures [25]. The derivations are exact in the spectral domain and approximate in the spatial domain, with really high accuracy obtained for paraxial beams. Direct integration of Maxwell equations [28] serve as a numerical illustration of the analytical expressions derived. In numerical simulations a dielectric constant equal two is assumed at the interface for the case of internal reflection. Only the case of beam transmission and normal incidence will be analyzed (cf. also [29])—beam reflection and arbitrary beam incidence can be treated on the same footing [28].

### A. Fundamental Gaussian beam

Let us start from the incident beam with its transverse field distribution  $\underline{E}_{(x,y)}^{(i)} = \hat{e}_{(x,y)} G$  and  $\underline{\tilde{E}}_{(x,y)}^{(i)} = \hat{e}_{(x,y)} \tilde{G}$  at the plane  $z = \text{const}$  in a form of the fundamental Gaussian function:

$$G(x, y, z) = \left[ \frac{w_w}{v(z)} \right]^2 \exp \left[ -\frac{1}{2} (x^2 + y^2) v^{-2}(z) \right], \quad (35)$$

$$\tilde{G}(k_x, k_y, z) = 2\pi \exp \left[ -\frac{1}{2} (k_x^2 + k_y^2) v^2(z) \right], \quad (36)$$

$$v^2(z) = w_w^2 (1 + iz z_D^{-1}), \quad (37)$$

specified by a position of the waist center, here at  $(x, y) = (0, 0)$ , a beam complex half width  $v$  and a diffraction length of the beam  $z_D = k^{(i)} w_w^2$ ,  $w_w$  being a beam (real) half width at the waist. The complex half width  $v$ ;  $v^{-2} = w^{-2} - iR^{-1}$ , defines two real quantities: the beam half width squared  $w^2 = w_w^2 (1 + z^2 z_D^{-2})$  and the radius of the phase-front curvature  $R = w_w^2 (z^{-1} z_D + z z_D^{-1})$ . Unit amplitude of the beam field at the beam center is assumed as a normalization condition for the fundamental, as well as for all higher-order, HG and LG beams. Note also that in all field expressions in (35)–(37) the longitudinal  $z$  coordinate can be normalized to  $z_D$  and the two,  $x$  and  $y$ , transverse coordinates can be normalized to  $w_w$ , respectively.

Higher-order HG and LG beams are considered here in their elegant version [11] and, thus, are hereafter referred to as the EHG and ELG beams. The beams are defined in the spatial domain by appropriate differentiation of the fundamental Gaussian field distribution (35)–(37). For the discussion of such definitions of the EHG and ELG beams, the

reader is referred to a recent report [30], where definitions of the, standard and elegant, HG and LG beams were rederived and compared. However, meanwhile the fundamental mode may be here defined in its transverse plane ( $x$ – $y$ ) or the interface plane  $X$ – $Y$ , the higher-order modes are defined only in the interface plane; that is, the projected definitions of the elegant beams will be used. For this reason, we also hereafter use the replacements in the notation in (34):  $G(x, y, z) \rightarrow G(X, Y, Z)$  and  $\tilde{G}(k_x, k_y, z) \rightarrow \tilde{G}(k_X, k_Y, Z)$ . All expressions for these beam modes are explicitly derived below.

### B. Elegant Hermite-Gaussian modes at the interface

Define the EHG mode  $G_{m,n}^{(EH)}$  of the order  $m+n$  by the partial  $X$  and  $Y$  derivatives of the order  $m$  and  $n$  in the horizontal and vertical directions, respectively, applied to the fundamental Gaussian [30]

$$\tilde{G}_{m,n}^{(EH)}(k_X, k_Y, Z) = (i w_w)^{m+n} k_X^m k_Y^n \tilde{G}(k_X, k_Y, Z), \quad (38)$$

$$G_{m,n}^{(EH)}(X, Y, Z) = w_w^{m+n} \partial_X^m \partial_Y^n G(X, Y, Z). \quad (39)$$

The definitions (38) and (39) are given here up to arbitrary normalization constant factor and imply a unit amplitude of the Gaussian beam at its waist center [cf. Eqs. (35)–(37)]. Hence, the partial derivatives  $\partial_X$  and  $\partial_Y$  increase the EHG mode indices  $m$  and  $n$  along the  $X$  and  $Y$  directions, respectively,

$$w_w \partial_X G_{m,n}^{(EH)}(X, Y, Z) = G_{m+1,n}^{(EH)}(X, Y, Z), \quad (40)$$

$$w_w \partial_Y G_{m,n}^{(EH)}(X, Y, Z) = G_{m,n+1}^{(EH)}(X, Y, Z), \quad (41)$$

and the transmission matrix (24) can be directly applied.

For the incident EHG beam of the TM polarization  $\underline{E}^{(i)} = \tilde{E}_X^{(i)} \hat{e}_X$ , with its spectral amplitude  $\tilde{E}_X^{(i)} = \tilde{G}_{m,n}^{(EH)}$ , or for the incident EHG beam of the TE polarization  $\underline{E}^{(i)} = \tilde{E}_Y^{(i)} \hat{e}_Y$ , with its spectral amplitude  $\tilde{E}_Y^{(i)} = \tilde{G}_{m,n}^{(EH)}$ , the transmitted beams become, respectively,

$$\begin{bmatrix} \tilde{E}_X^{(t)} \\ \tilde{E}_Y^{(t)} \end{bmatrix}_{TM} = \frac{1}{2} (\eta t_p + t_s) \begin{bmatrix} \tilde{G}_{m,n}^{(EH)} \\ 0 \end{bmatrix} - (\eta t_p - t_s) \times (k_{\perp} w_w)^{-2} \begin{bmatrix} 0 \\ \tilde{G}_{m+1,n+1}^{(EH)} \end{bmatrix} + \begin{bmatrix} \tilde{\delta}_X \\ \tilde{\delta}_Y \end{bmatrix}_{TM}, \quad (42)$$

$$\begin{bmatrix} \tilde{E}_X^{(t)} \\ \tilde{E}_Y^{(t)} \end{bmatrix}_{TE} = \frac{1}{2} (\eta t_p + t_s) \begin{bmatrix} 0 \\ \tilde{G}_{m,n}^{(EH)} \end{bmatrix} - (\eta t_p - t_s) \times (k_{\perp} w_w)^{-2} \begin{bmatrix} \tilde{G}_{m+1,n+1}^{(EH)} \\ 0 \end{bmatrix} + \begin{bmatrix} \tilde{\delta}_X \\ \tilde{\delta}_Y \end{bmatrix}_{TE}. \quad (43)$$

In Eqs. (42) and (43), the labels  $TM$  and  $TE$  indicate the type of polarization of the incident beam and

$$\begin{bmatrix} \tilde{\delta}_X \\ \tilde{\delta}_Y \end{bmatrix}_{TM} = -\frac{1}{2} (\eta t_p - t_s) (k_{\perp} w_w)^{-2} \begin{bmatrix} \tilde{G}_{m+2,n}^{(EH)} - \tilde{G}_{m,n+2}^{(EH)} \\ 0 \end{bmatrix}, \quad (44)$$

$$\begin{bmatrix} \tilde{\delta}_X \\ \tilde{\delta}_Y \end{bmatrix}_{TE} = + \frac{1}{2} (\eta_p - t_s) (k_{\perp} w_w)^{-2} \begin{bmatrix} 0 \\ \tilde{G}_{m+2,n}^{(EH)} - \tilde{G}_{m,n+2}^{(EH)} \end{bmatrix}. \quad (45)$$

As for the normal, or close to normal, incidence the term  $\eta_p - t_s$  is much less than  $\eta_p + t_s$ , the contributions  $\tilde{\delta}_{TM}$  and  $\tilde{\delta}_{TE}$  in Eqs. (42) and (43), will be further neglected. This approximation is quite reasonable under paraxial approximation assumption, that is roughly for  $k^{(i)} w_w > 2\pi$ . Equations (44) and (45) indicate that the transmitted beams attain finite values also in the polarization components opposite to those of the incident beam. They are approximately EHG beams with their indices being increased, with respect to the incident beam, by one along both,  $X$  and  $Y$ , transverse directions.

On the grounds of Eq. (26), one index (in  $X$  or  $Y$  direction) is further increased by one in the longitudinal field component

$$\begin{aligned} \tilde{E}_Z^{(i)}|_{TM} &\cong i(2w_w k_Z^{(i)})^{-1} [(\eta_p + t_s) \tilde{G}_{m+1,n}^{(EH)} \\ &\quad - 2(\eta_p - t_s) (k_{\perp} w_w)^{-2} \tilde{G}_{m+1,n+2}^{(EH)}], \end{aligned} \quad (46)$$

$$\begin{aligned} \tilde{E}_Z^{(i)}|_{TE} &\cong i(2w_w k_Z^{(i)})^{-1} [(\eta_p + t_s) \tilde{G}_{m,n+1}^{(EH)} \\ &\quad - 2(\eta_p - t_s) (k_{\perp} w_w)^{-2} \tilde{G}_{m+2,n+1}^{(EH)}]. \end{aligned} \quad (47)$$

For normal or close to normal incidence in the paraxial range, the longitudinal field components in Eqs. (46) and (47) are approximately proportional to the term  $\eta_p + t_s$ . Therefore, the spatial shape of the  $Z$  component of the transmitted beam follows the spatial shape of the  $Z$  component of the incident beam. Moreover  $\tilde{E}_Z^{(i)}|_{TM} \cong t_Z^{(EH)} \tilde{E}_Z^{(i)}|_{TM}$  and  $\tilde{E}_Z^{(i)}|_{TE} \cong t_Z^{(EH)} \tilde{E}_Z^{(i)}|_{TE}$ , where  $t_Z^{(EH)} = \frac{1}{2} (\eta_p + t_s) k_Z^{(i)} / k_Z^{(i)}$  may be regarded as the transmission coefficient of the  $Z$  component of the EHG beam.

Beam field distribution in the spatial domain can be now obtained by analytical evaluation, after substitution Eqs. (42) and (43) to the representation (34), or by direct numerical integration of Maxwell equations. The numerical approach was described and demonstrated in [28] for critical incidence of TIR. In analytic evaluation of (34), for normal incidence of paraxial beams, the Fresnel coefficients can be evaluated at  $\vartheta^{(i)} = 0$ . Field intensity plots are presented in Figs. 2 and 3, for  $k^{(i)} w_w = 2\pi$ , that is for two wavelengths in the beam diameter at its waist, and for normal incidence of the EHG<sub>1,1</sub> beam with the indices in the  $X$  and  $Y$  directions equal 1.

The incident beam of the EHG<sub>1,1</sub> spatial pattern and of TM polarization is shown in Fig. 2(a), the pattern of the transmitted beam component of the opposite, TE polarization is shown in Fig. 2(b). The plots clearly confirm predictions of Eq. (42); the pattern of the TE transmitted field component is of the EHG<sub>2,2</sub> spatial shape. Note that for normal incidence the case is symmetric in  $X$  and  $Y$  coordinates, for the TE polarization of the incident beam, the TM component of the transmitted beam possesses the same EHG<sub>2,2</sub> pattern as that of the TE component of the transmitted beam for the TM polarization of the incident beam. The interface, however, still differentiates these two cases in the longitudinal,  $Z$

components of the transmitted beams as it is shown in Fig. 3. The  $Z$  component of the transmitted beam exhibits the EHG<sub>2,1</sub> pattern for incident TM polarization, as shown in Fig. 3(a), and the EHG<sub>1,2</sub> pattern for incident TE polarization, as shown in Fig. 3(b). Figure 3 entirely confirm theoretical predictions of Eqs. (46) and (47).

### C. Elegant Laguerre-Gaussian modes at the interface

Let us turn now into the case of beams of a cylindrical symmetry and describe them in the cylindrical reference frames  $Or_{\perp}\psi Z$  and  $Ok_{\perp}\varphi k_Z^{(b)}$  in the spatial and spectral domains, respectively, where  $X = r_{\perp} \cos \psi$ ,  $Y = r_{\perp} \sin \psi$ ,  $k_X = k_{\perp} \cos \varphi$  and  $k_Y = k_{\perp} \sin \varphi$ . Action of the interface on the incident beams can be then described more compactly in new frames  $Os\bar{s}Z$  and  $O\kappa\bar{\kappa}Z$  of complex coordinates and their complex conjugates (denoted by the overbar). These coordinates are defined in the spatial domain

$$\varsigma = 2^{-1/2}(X + iY), \quad \partial_{\varsigma} = 2^{-1/2}(\partial_X - i\partial_Y), \quad (48)$$

where  $\varsigma\bar{\varsigma} = 2^{-1}r_{\perp}^2$  and  $\partial_{\varsigma}\partial_{\bar{\varsigma}} = 2^{-1}(\partial_X^2 + \partial_Y^2)$ , and in the spectral domain

$$\kappa = 2^{-1/2}(k_X + ik_Y), \quad \partial_{\kappa} = 2^{-1/2}(\partial_{k_X} - i\partial_{k_Y}), \quad (49)$$

where  $\kappa\bar{\kappa} = 2^{-1}k_{\perp}^2$  and  $\partial_{\kappa}\partial_{\bar{\kappa}} = 2^{-1}(\partial_{k_X}^2 + \partial_{k_Y}^2)$ . Note that in cylindrical coordinates  $\varsigma = 2^{-1/2}r_{\perp} \exp(i\psi)$ ,  $\kappa = 2^{-1/2}k_{\perp} \exp(i\varphi)$ . The fundamental Gaussian (35) and (36) now reads  $G(\varsigma, \bar{\varsigma}, Z) = (w_w/v)^2 \exp(-\varsigma\bar{\varsigma}v^{-2})$  and  $\tilde{G}(\kappa, \bar{\kappa}, Z) = 2\pi \exp(-\kappa\bar{\kappa}v^2)$  and the beam representation (34), with new dependence on the new complex coordinates, yields

$$\begin{aligned} \underline{E}^{(b)}(\varsigma, \bar{\varsigma}, Z) &= \left(\frac{w_w}{2\pi}\right)^2 \exp(\pm ik^{(b)}z) i \int d\kappa \int d\bar{\kappa} \tilde{E}^{(b)} \\ &\quad \times (\kappa, \bar{\kappa}, Z) \exp[i(\varsigma\bar{\kappa} + \bar{\varsigma}\kappa)], \end{aligned} \quad (50)$$

where  $\varsigma\bar{\kappa} + \bar{\varsigma}\kappa = k_{\perp} r_{\perp} \cos(\psi - \varphi)$ .

Next, define at the interface plane  $X-Y$  the ELG beam of the order  $2p+l$  in the similar manner as it has been done for the EHG beams in the spectral domain

$$\tilde{G}_{p,l}^{(EL)}(\kappa, \bar{\kappa}, Z) = (iw_w)^{2p+l} \kappa^{p+l} \bar{\kappa}^p \tilde{G}(\kappa, \bar{\kappa}, Z), \quad (51)$$

where integers  $p$  and  $l$  are the radial and azimuthal non-negative indices of the ELG beam [30]. In the spatial domain, the definition (51) yields

$$G_{p,l}^{(EL)}(\varsigma, \bar{\varsigma}, Z) = w_w^{2p+l} \partial_{\varsigma}^{2p+l} \partial_{\bar{\varsigma}}^p G(\varsigma, \bar{\varsigma}, Z). \quad (52)$$

For negative values of  $l$  Eqs. (51) and (52) yield  $\tilde{G}_{p,l}^{(EL)}(\kappa, \bar{\kappa}, Z) = \tilde{G}_{p,-l}^{(EL)}(\bar{\kappa}, \kappa, Z)$  and  $G_{p,l}^{(EL)}(\varsigma, \bar{\varsigma}, Z) = G_{p,-l}^{(EL)}(\bar{\varsigma}, \varsigma, Z)$ . Note also that  $\kappa^{p+l} \bar{\kappa}^p = (2^{-1/2}k_{\perp})^{2p+l} \exp(il\varphi)$ . Hence, the definition (51) directly implies changes in the indices of the ELG beams under transmission

$$\tilde{G}_{p,l}^{(EL)}(\kappa, \bar{\kappa}, Z) \exp(\pm 2i\varphi) = \tilde{G}_{p\pm 1, l\pm 2}^{(EL)}(\kappa, \bar{\kappa}, Z), \quad (53)$$

$$\tilde{G}_{p,l}^{(EL)}(\kappa, \bar{\kappa}, Z) \exp(\pm i\varphi) = \tilde{G}_{p\pm 1/2, l\pm 1}^{(EL)}(\kappa, \bar{\kappa}, Z), \quad (54)$$

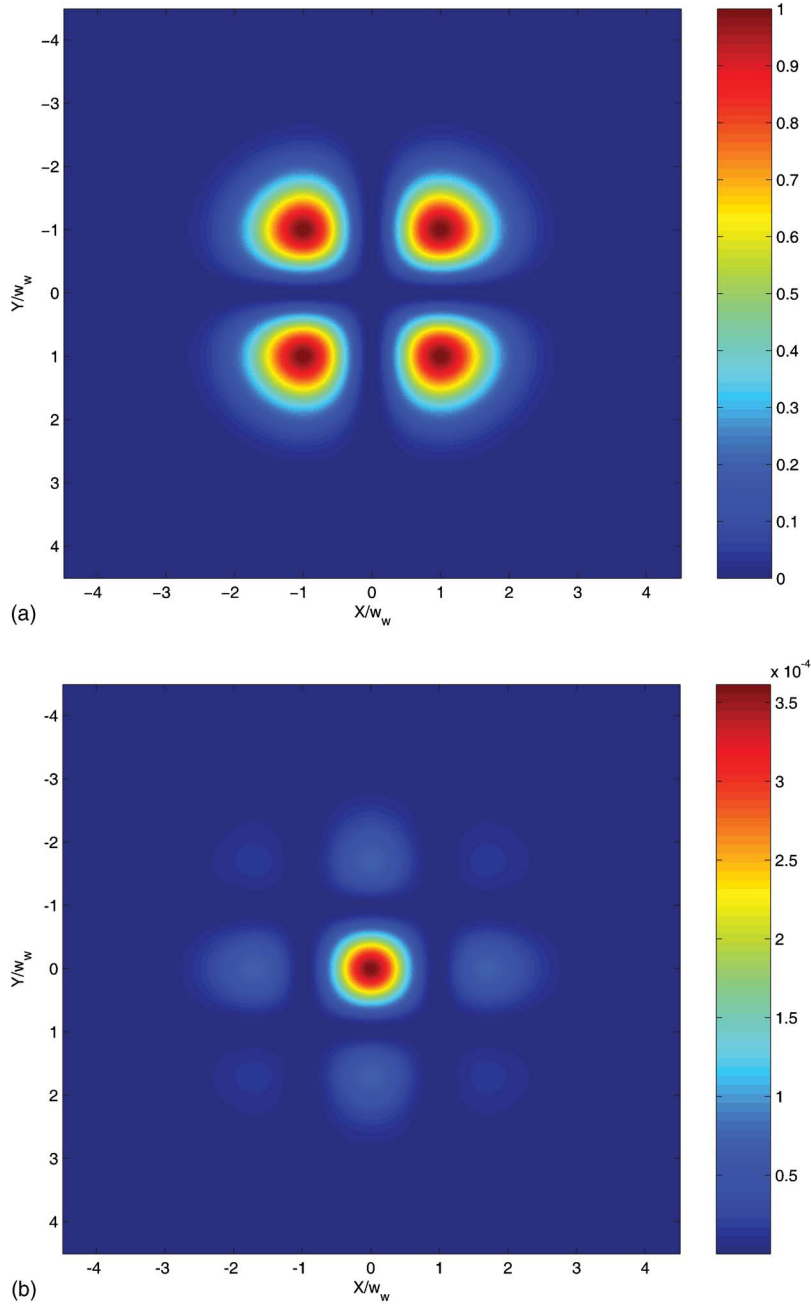


FIG. 2. (Color online) Beam intensity transverse distribution of the EHG beam at the interface; the incident beam of the  $\text{EHG}_{1,1}$  pattern and of TM polarization (a) and the transmitted beam TE component of the  $\text{EHG}_{2,2}$  pattern (b);  $X$  and  $Y$  coordinates normalized to  $w_w$ , normal incidence,  $k^{(i)}w_w = 2\pi$ .

including also fractional values admitted in the radial indices of the ELG beams. Eqs. (53) and (54) are central results of this section. They lead to exact description of the LG beams of circular polarization interacting with the interface, as will be shown below.

Let the incident beam be of the ELG shape with its spectral amplitude  $\tilde{E}_R^{(i)} = \tilde{G}_{p,l}^{(EL)}$  for the CR polarization, i.e., for  $\underline{E}^{(i)} = \tilde{E}_R^{(i)} \hat{e}_R$ , or with its spectral amplitude  $\tilde{E}_L^{(i)} = \tilde{G}_{p,l}^{(EL)}$  for the CL polarization, i.e., for  $\underline{E}^{(i)} = \tilde{E}_L^{(i)} \hat{e}_L$ , respectively. Then the rules (53) and (54), together with the definition of the transmission matrix (32), lead in the spectral domain to exact evaluation of the transmitted ELG beams at the interface, with the following outcome:

$$\begin{bmatrix} \tilde{E}_R^{(t)} \\ \tilde{E}_L^{(t)} \end{bmatrix}_{CR} = \frac{1}{2}(\eta t_p + t_s) \begin{bmatrix} \tilde{G}_{p,l}^{(EL)} \\ 0 \end{bmatrix} + \frac{1}{2}(\eta t_p - t_s) \begin{bmatrix} 0 \\ \tilde{G}_{p-1,l+2}^{(EL)} \end{bmatrix}, \quad (55)$$

$$\begin{bmatrix} \tilde{E}_R^{(t)} \\ \tilde{E}_L^{(t)} \end{bmatrix}_{CL} = \frac{1}{2}(\eta t_p + t_s) \begin{bmatrix} 0 \\ \tilde{G}_{p,l}^{(EL)} \end{bmatrix} + \frac{1}{2}(\eta t_p - t_s) \begin{bmatrix} \tilde{G}_{p+1,l-2}^{(EL)} \\ 0 \end{bmatrix}, \quad (56)$$

for the CR and CL polarization of the incident beam, respectively. Similarly, the longitudinal components of the incident beams are of the form  $\tilde{E}_Z^{(i)} = -2^{-1/2} \tilde{G}_{p-1/2,l+1}^{(EL)} \tan \vartheta^{(i)}$  for the

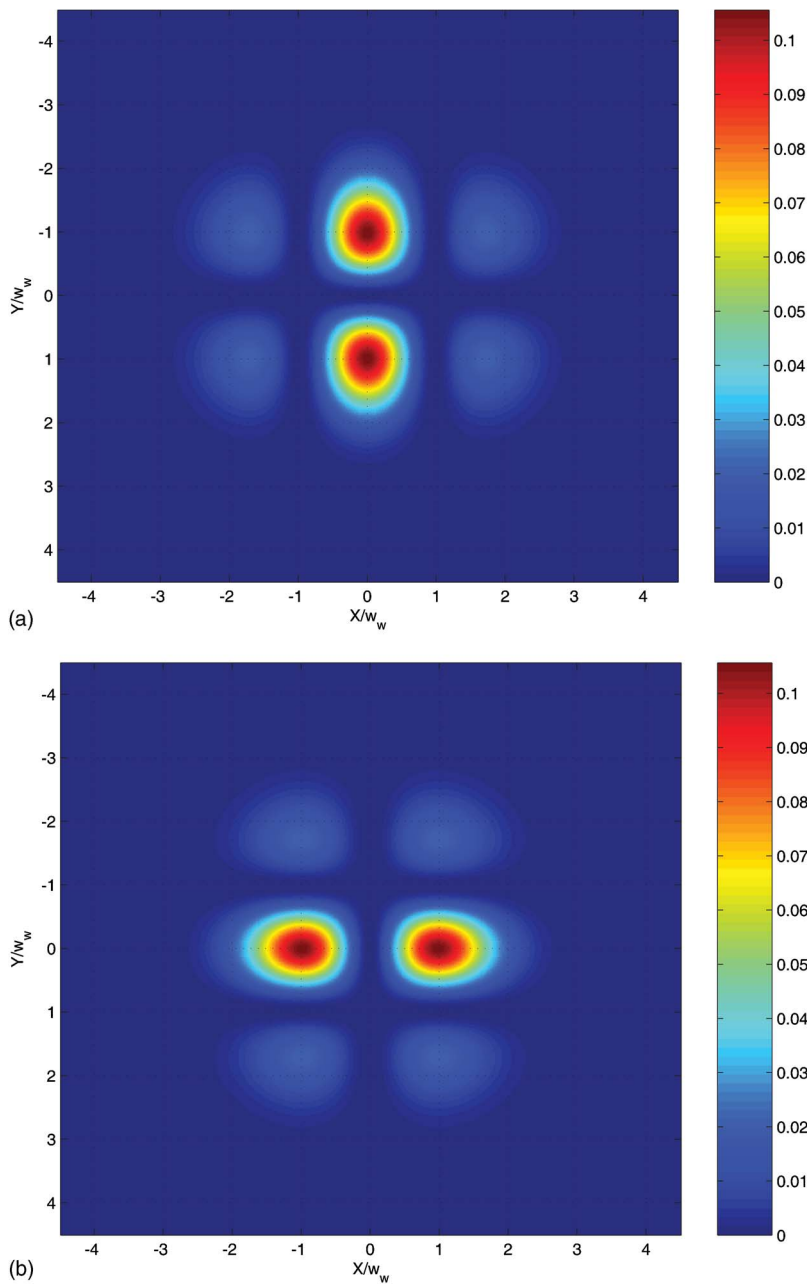


FIG. 3. (Color online) Beam intensity transverse distribution of the EHG beam at the interface; the Z component of the transmitted beam of the  $\text{EHG}_{2,1}$  pattern for the incident  $\text{EHG}_{1,1}$  beam of TM polarization (a) and the Z component of the transmitted beam of the  $\text{EHG}_{1,2}$  pattern for the incident  $\text{EHG}_{1,1}$  beam of TE polarization (b); normal incidence,  $k^{(i)}_{W_w} = 2\pi$ .

CR polarization and  $\tilde{E}_Z^{(i)} = -2^{-1/2} \tilde{G}_{p+1/2, l-1}^{(EL)} \tan \vartheta^{(i)}$  for the CL polarization and that yields for the transmitted beam, respectively,

$$\tilde{E}_Z^{(t)}|_{CR} = -2^{-1/2} \eta t_p \tan \vartheta^{(t)} \tilde{G}_{p-1/2, l+1}^{(EL)}, \quad (57)$$

$$\tilde{E}_Z^{(t)}|_{CL} = -2^{-1/2} \eta t_p \tan \vartheta^{(t)} \tilde{G}_{p+1/2, l-1}^{(EL)}. \quad (58)$$

Therefore, the Z components of the transmitted beams, i.e.,  $\tilde{E}_Z^{(t)} = t_Z^{(EL)} \tilde{E}_Z^{(i)}$ , with the transmission coefficient  $t_Z^{(EL)} = \eta t_p \tan \vartheta^{(t)} / \tan \vartheta^{(i)}$ , possess the same topological charge  $l \pm 1$  as the incident beam [cf. also Eq. (31)]. Note that, contrary to the EHG beam case, all expressions derived above in the spectral domain for ELG beams are exact and the longi-

tudinal field component resolves into *one* ELG beam function with fractional value  $p \mp 1/2$  of the radial index.

The interface changes indices of the incident ELG beam in the opposite transverse field component. For the incident CR (CL) polarization the radial index of the beam mode decreases (increases) by one and the azimuthal index increases (decreases) by two in the CL (CR) polarization component of the transmitted beam. In the longitudinal field component, the radial index decreases (increases) by half and the azimuthal index increases (decreases) by one with respect to the indices of the transverse component of the incident ELG beam of the CR (CL) polarization. Examples of the ELG beam transverse field distribution at the interface is presented in Figs. 4–7 for narrow beams ( $k^{(i)}_{W_w} = 2\pi$ ). Incidence always is normal and the incident beam always has a pattern of the  $\text{ELG}_{1,3}$  function.

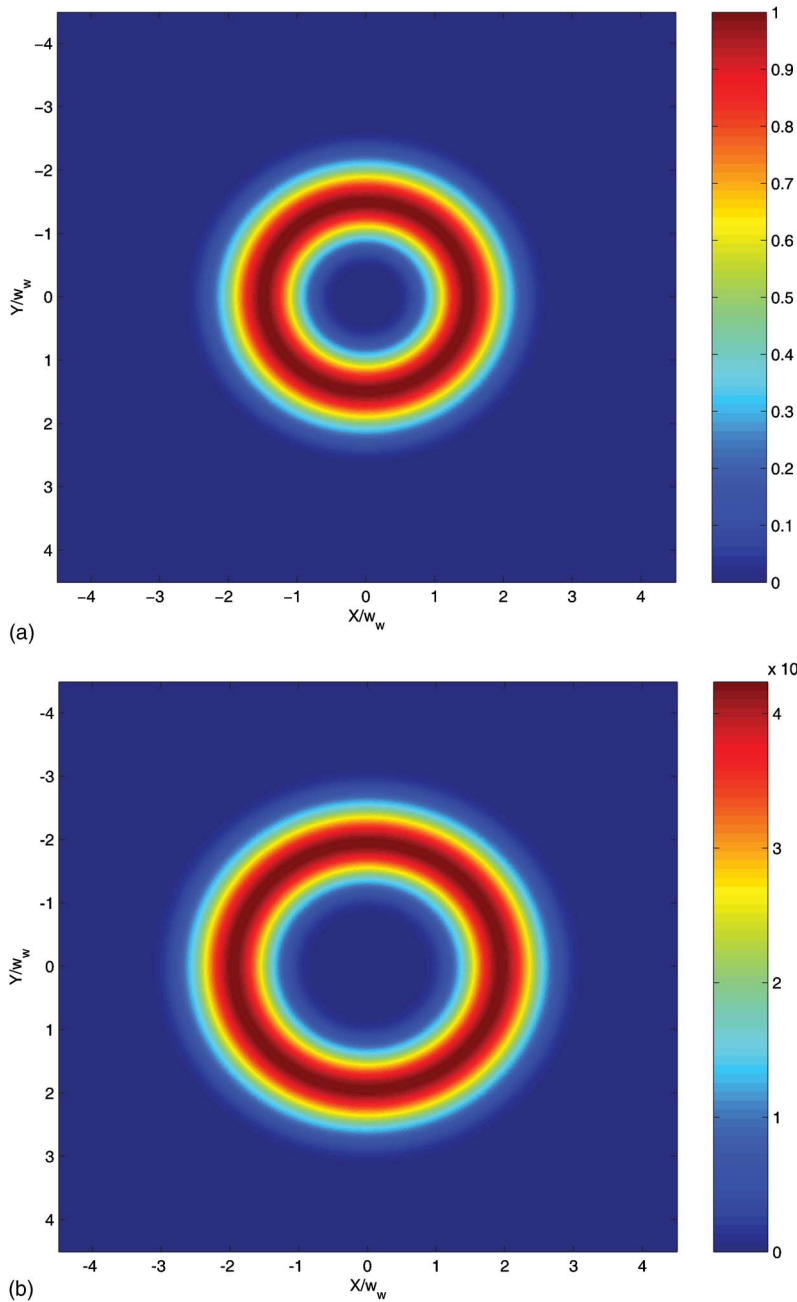


FIG. 4. (Color online) Beam intensity transverse distribution of the ELG beam at the interface; the incident beam of the  $ELG_{1,3}$  pattern and of CR polarization (a) and the transmitted beam CL component of the  $ELG_{0,5}$  pattern (b); normal incidence,  $k^{(i)}w_w = 2\pi$ .

Figures 4 and 5 display intensity profiles of the ELG beams. The profile of the incident beam of the  $ELG_{1,3}$  pattern and of CR polarization is displayed in Fig. 4(a) and that of the CL component of the  $ELG_{0,5}$  pattern of the transmitted beam is shown in Fig. 4(b). The profile of the incident beam of the  $ELG_{1,3}$  pattern and of CL polarization is displayed in Fig. 5(a) and that of the CR component of the  $ELG_{2,1}$  pattern of the transmitted beam is shown in Fig. 5(b). Dependence of a number and radii of the beam annular rings on the incident beam polarization and azimuthal index  $l$  is clearly vivid. However, a value of the radial index remains uncertain due to a limited accuracy of the numerical integration for points of diminishing intensity of the beams.

Also, nothing specific can be inferred from Figs. 4 and 5 about the azimuthal indices of the beams. The intensity profiles are not sufficient to describe beams of complex struc-

ture, especially the beams with singularities in their phase fronts. To complete these figures, phase patterns of the incident and transmitted beams are drawn in Figs. 6–8. Values of the azimuthal index are counted as the number of  $2\pi$  cycles in phase around the beam axis. This number distinguishes the ELG phase patterns of the beams shown in these figures.

The phase transverse distribution of the incident  $ELG_{1,3}$  beam of CR polarization is shown in Fig. 6(a), the phase of the transmitted beam component of the opposite, CL polarization is shown in Fig. 6(b)—its pattern is of the  $ELG_{0,5}$  function. On the other hand, even for normal incidence this case is not symmetric with respect to the replacement of CR polarization by CL polarization in the incident beam—values of the SAM about the  $Z$  axis have opposite signs in these two cases. Therefore, the beam incidence of CL polarization is

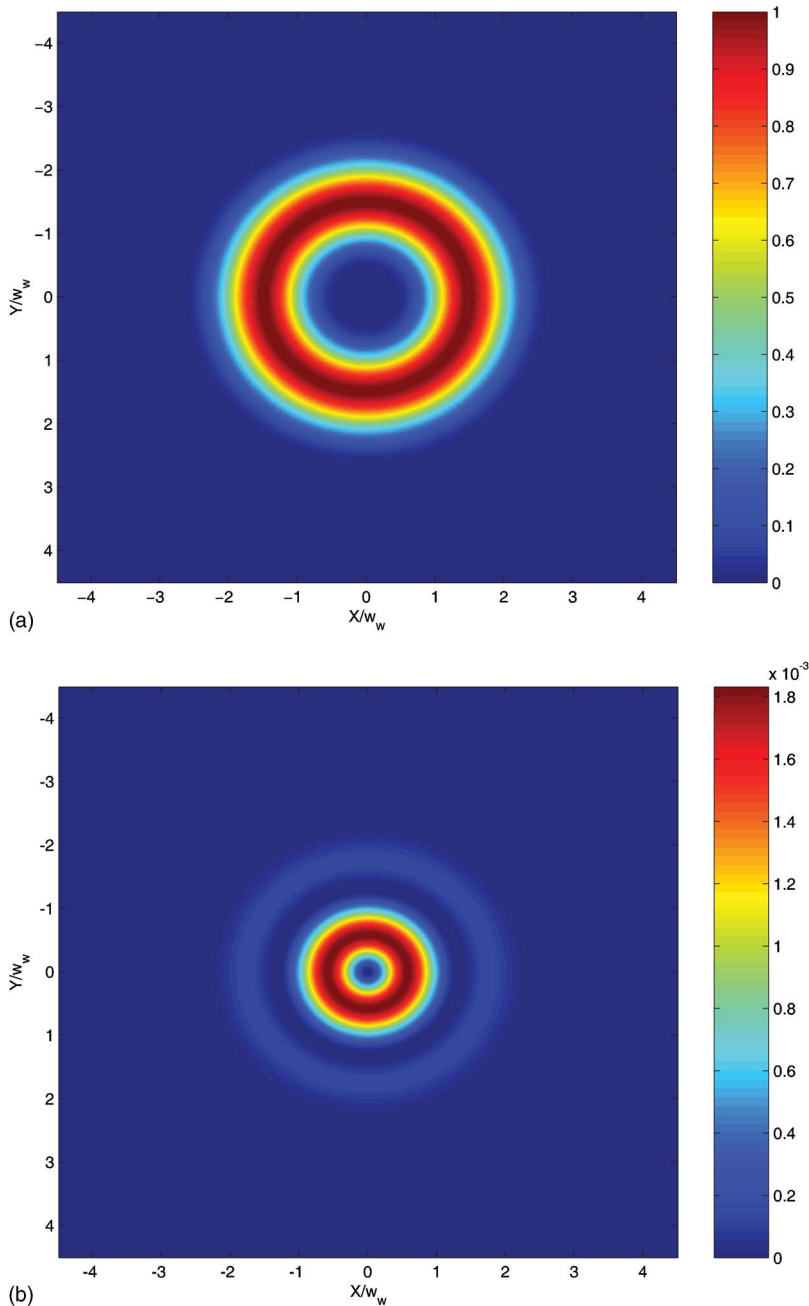


FIG. 5. (Color online) Beam intensity transverse distribution of the ELG beam at the interface; the incident beam of the  $ELG_{1,3}$  pattern and of CL polarization (a) and the transmitted beam CR component of the  $ELG_{2,2}$  pattern (b); normal incidence,  $k^{(i)}w_w = 2\pi$ .

also described in Fig. 7. The phase of the incident  $ELG_{1,3}$  beam is shown in Fig. 7(a) and the phase of the CR component of the transmitted beam of the  $ELG_{2,1}$  shape is shown in Fig. 7(b).

Figures 6 and 7 confirm predictions of Eqs. (55) and (56) concerning the phase distribution of the beams. However, Figs. 6(b) and 7(b) display additional ring of zero field amplitude far away from the beam axes. This discrepancy between numerical results and theoretical predictions might be originated by the approximation assumed in evaluation of the Fresnel coefficients (at the beam mean direction) in the field representation (34) or by limited accuracy of the numerical evaluation of this equation for points of diminishing intensity of the beam fields. Note, however, that the beam phase or the azimuthal index  $l$ , not the beam magnitude or radial index  $p$ , is usually used in sorting the beam modes [21].

Figure 8 shows the phase distribution of the longitudinal field components predicted by Eqs. (57) and (58). For the CR polarization of the incident beam of the  $ELG_{1,3}$  shape, Fig. 8(a) displays the phase distribution for the longitudinal field component of the transmitted beam—that is of the pattern of the  $ELG_{1/2,4}$  function. For CL polarization of the incident beam of the same shape  $ELG_{1,3}$  the phase of the transmitted beam changes to the  $ELG_{3/2,2}$  function as shown in Fig. 8(b). For both these polarization states of the incident ELG beam, the phase structure of the Z components of the transmitted, and the reflected as well, beams appears the same as that of the incident beams.

As numerical simulations applied in this section are based on direct integration of Maxwell equations [28], the examples of beam intensity and phase distribution at the interface, as shown in Figs. 2–8, evidently confirm theoretical

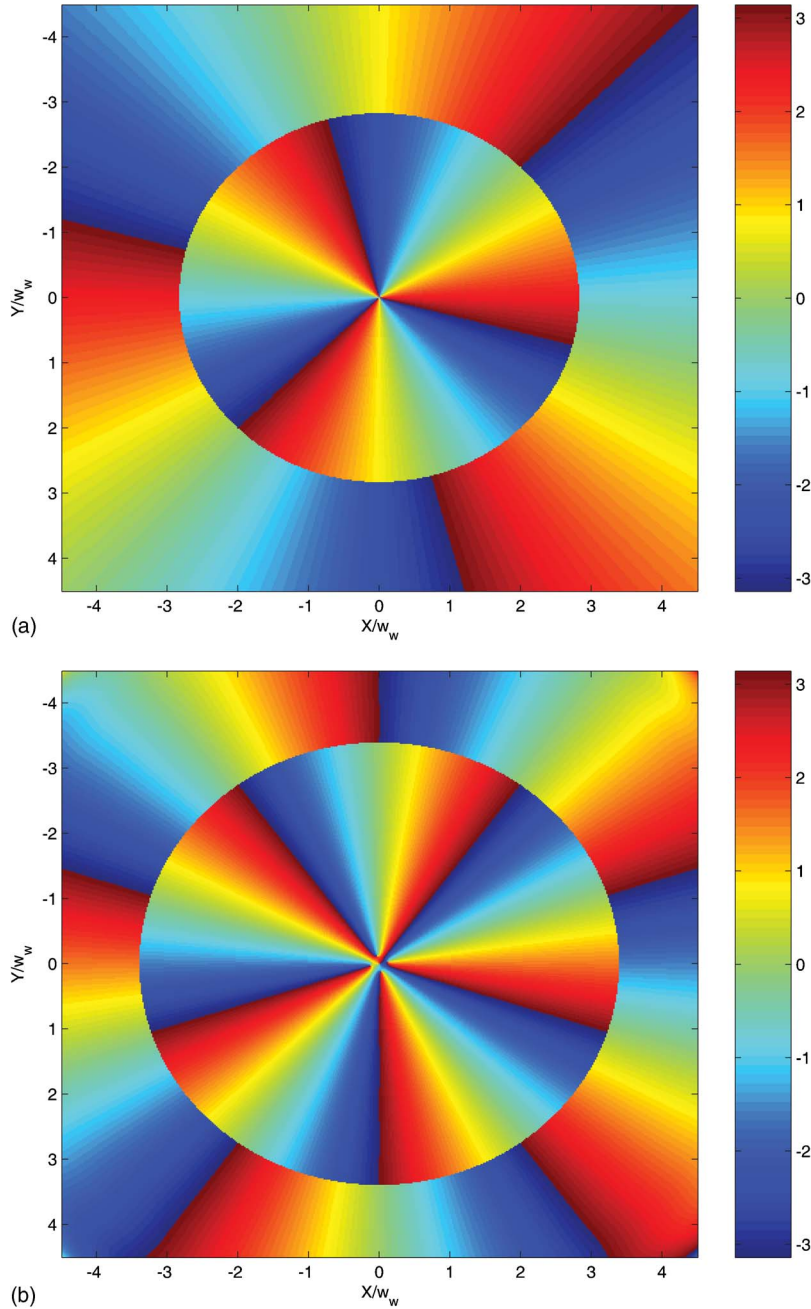


FIG. 6. (Color online) Phase transverse distribution of the ELG beam at the interface; the incident  $ELG_{1,3}$  beam of CR polarization (a) and the transmitted beam CL component of the  $ELG_{0,5}$  pattern (b); normal incidence,  $k^{(i)}w_w = 2\pi$ .

predictions given by analytical expressions (42)–(47) for EHG beams and (55)–(58) for ELG beams. Efficiency of the XPS effect can be estimated from the expressions (24), (25), (32), and (33) for the beam field and its amplitudes (22) and (23) in the spectral domain. The standard Fresnel coefficients are there replaced by their partial counterparts:  $t_{(p,s)}^{(DP)} = \frac{1}{2}(\eta t_p + t_s)$  and  $r_{(p,s)}^{(DP)} = \frac{1}{2}(r_p - r_s)$  of the direct polarization (DP), that is that of the incident beam, and  $t_{(p,s)}^{(XP)} = \frac{1}{2}(\eta t_p - t_s)$  and  $r_{(p,s)}^{(XP)} = \frac{1}{2}(r_p + r_s)$  of the opposite polarization (XP), which is that produced by the XPC effect. The DP and XP coefficients do not depend on the incident beam polarization. They are interrelated at the interface by the field continuity relations  $t_{(p,s)}^{(DP)} = 1 - r_{(p,s)}^{(DP)}$  and  $t_{(p,s)}^{(XP)} = -r_{(p,s)}^{(XP)}$  separately for the beam components of opposite polarization of the transmitted

beams—TM or TE for EHG beams and CR or CL for ELG beams.

The efficiency of the XPC effect is determined by the ratio  $t_{(p,s)}^{(XP)}/t_{(p,s)}^{(DP)}$ , here given for beam transmission. For normal incidence this ratio is small—of the order  $10^{-2}$ . On the other hand, for beam reflection at critical incidence, magnitude of the ratio  $r_{(p,s)}^{(XP)}/r_{(p,s)}^{(DP)}$  is about two orders greater, as expected. However, the case of critical incidence does not seem satisfactory for the ELG beam incidence, as the cylindrical symmetry of the beam-interface configuration becomes then broken and the beams become deformed. Therefore, the problem of the efficiency of the XPC effect for beam normal incidence still remains to be solved. It seems that a planar boundary of a doubly negative medium [31–33] may appear to be a proper solution to this problem.

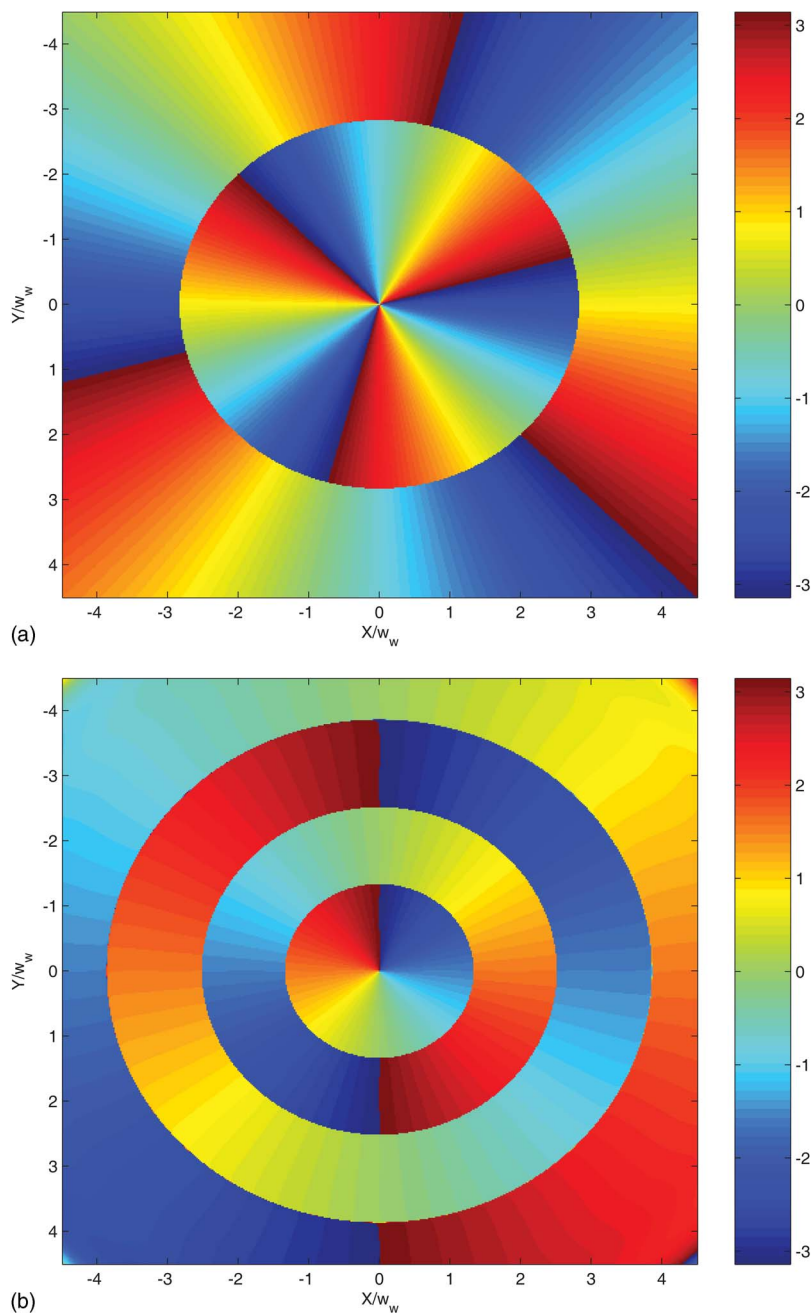


FIG. 7. (Color online) Phase transverse distribution of the ELG beam at the interface; the incident  $ELG_{1,3}$  beam of CL polarization (a) and the transmitted beam CR component of the  $ELG_{2,1}$  pattern (b); normal incidence,  $k^{(i)}w_w = 2\pi$ .

#### D. Beam normal modes at the interface

Within the paraxial approximation, the scalar HG and LG functions are solutions of the scalar wave equation. The vector HG and LG beams are paraxial solutions of the Maxwell equations and build two orthogonal basis sets for any paraxial beam mode of free propagation. In the analysis presented in this section these sets comply four additional conditions, that is the vector (HG and LG) Gaussians: (i) should be considered in their elegant version, (ii) their vectorial form should be defined in the linear (TE/TM) basis for the EHG beams, (iii) their vectorial form should be defined in the circular (CR/CL) basis of the ELG beams, and (iv) the beams should be defined with respect to the interface plane. That is, at least for beams other than the fundamental Gaussian, their spatial and polarization structures should be defined

in the interface plane  $X-Y$ , and not, as usual, in the beam transverse plane  $x-y$ .

The HG and LG beams, which obey the conditions (i)–(iv), that is the projected EHG and ELG beams, may be regarded as normal modes of vector beams at the interface. For any member of one from these two sets incident on the interface, the reflected and transmitted beams also belong to this set. The beams are defined by one pair of their spatial indices— $m$  and  $n$  for the EHG beam or  $p$  and  $l$  for the ELG beam, in each of the two opposite beam polarizations—TM and TE or CR and CL for the EHG or ELG beam, respectively. The interface acts almost exactly in this manner. For ELG beams, only one approximation necessary in the derivations above was assumed in the spatial domain, concerning mean values of the Fresnel coefficients. Still even this as-

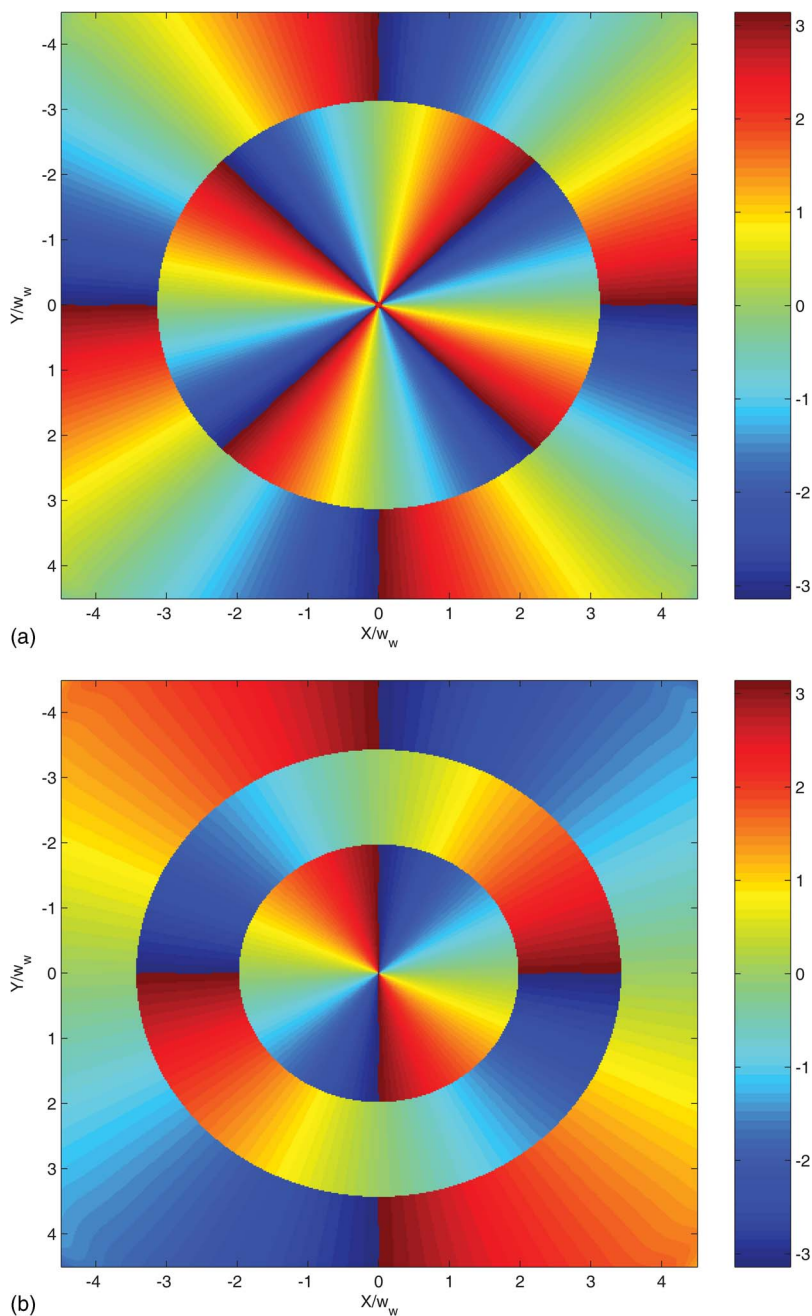


FIG. 8. (Color online) Phase transverse distribution of the ELG beam at the interface; the transmitted beam Z component of the  $ELG_{1/2,4}$  pattern for the incidence of the  $ELG_{1,3}$  beam of CR polarization (a), the transmitted beam Z component of the  $ELG_{3/2,2}$  pattern for the incidence of the  $ELG_{1,3}$  beam of CL polarization (a); normal incidence,  $k^{(i)}w_w=2\pi$ .

sumption can be neglected if nonuniform polarization of the beams is admitted.

The interface redistributes incident energy, momentum, and angular momentum into a pair of beams of two orthogonal polarization states, one pair for each of the transmitted and reflected beams. One element of this pair possesses the same polarization and spatial structure as those of the incident beam. The spatial structure of the second element, that of the opposite polarization, appears also spatially biorthogonal to the first element. This process may be understood as creation and annihilation of beam modes at the planar interface. For ELG beams, it also means creation and annihilation of optical vortices placed on axes of these beams.

Having defined the biorthogonal sets of normal modes defined above, any field with arbitrary complex amplitude

and polarization distribution can be readily expanded in a standard manner in terms of these modes. Until now EHG and ELG beams have been used mainly in the context of propagation in the free-space, infinite bulk material, or non-self-adjoint optical systems [34,35]. This contribution provides, to the best of my knowledge, first analytical and exact derivation of the decomposition of an arbitrary 3D beam field at the planar interface in terms of the (projected) elegant HG and LG normal beam modes.

### V. ANGULAR MOMENTUM OF BEAMS AT THE INTERFACE

Let now look into the beam transmission from a slightly different point of view. It is well known that beams carry

TAM composed, in general, of SAM and OAM components [1]. The spin component is associated with beam polarization and the orbital component results from azimuthal transverse distribution of beam phase. For the circularly polarized beams, the SAM component is equal to  $\sigma\hbar$  per photon, where  $\sigma=\pm 1$  for the CR and CL polarization, respectively. Since the LG beams are angular momentum eigenstates, their OAM component, associated with the beam phase dependence of the form  $\exp(il\psi)$ , is equal to  $l\hbar$  per photon. Both SAM and OAM contribute to the  $Z$  component of TAM per photon

$$j_Z^{(b)} = (\sigma + l)\hbar, \quad (59)$$

separately for the incident ( $b=i$ ), transmitted ( $b=t$ ), and reflected ( $b=r$ ) beams, where for any beam the angular momentum is measured with respect to the normal to the interface (the  $Z$  axis). Equations (55) and (56) show that TAM per photon is conserved for ELG beam transmission at the interface, and similarly also for ELG beam reflection. For any photon, transmitted or reflected at the interface, its TAM is conserved

$$j_Z^{(i)} = j_Z^{(t)} \quad \text{or} \quad j_Z^{(i)} = j_Z^{(r)}, \quad (60)$$

respectively. Therefore, the SAM and OAM components of TAM per photon depend of the polarization of the transmitted beam.

For example, for a single photon of the incident beam  $\tilde{E}_R^{(i)} = \tilde{G}_{p,l}^{(EL)} \hat{e}_R$ , of the topological charge  $l$  and of the CR polarization ( $\sigma=1$ ), its TAM amounts  $j_Z^{(i)} = l+1$ . The transmitted (or the reflected) photon possess the same TAM  $j_Z^{(t)} = l+1$  independently of its polarization [cf. Eq. (55)]. For the transmitted photon of the CR polarization, its spin and orbital components are the same as those of the incident photon. However, for the opposite, CL polarization of the transmitted beam the OAM of the photon is increased by two (from  $l$  to  $l+2$ ) as its SAM is decreased at the same time by two (from  $\sigma=1$  to  $\sigma=-1$ ).

Similar rules are also valid for the incident ELG beams  $\tilde{E}_L^{(i)} = \tilde{G}_{p,l}^{(EL)} \hat{e}_L$  of the CL polarization ( $\sigma=-1$ ). The TAM  $j_Z^{(i)} = l-1$  per photon, as well the SAM  $\sigma=-1$  and OAM  $l$  per photon, of the transmitted beam of the same, CL polarization appears the same as the TAM, SAM, and OAM of the incident photon [cf. Eq. (56)]. For the transmitted photon of the opposite, CR polarization its OAM is decreased by two (from  $l$  to  $l-2$ ) as its SAM is increased at the same time also by two (from  $\sigma=-1$  to  $\sigma=1$ ). Therefore, its TAM  $j_Z^{(i)} = l-1$  per photon remains equal to that of the photon of the incident ELG beam.

Equations (55) and (56), together with their counterparts for beam reflection, may be regarded as equivalent to the conservation principle of TAM for a single photon at the flat interface. With the continuity relations (22) and (23), they correspond also to the conservation of integrated TAM  $J_Z^{(b)} = j_Z^{(b)} N^{(b)}$  of any set of the (incident, refracted, and reflected) projected ELG beams at the interface

$$J_Z^{(i)} = J_Z^{(t)} + J_Z^{(r)}, \quad (61)$$

where  $N^{(b)} = U^{(b)}/\hbar\omega$  stands for a number of photons in a monochromatic beam of time averaged energy  $U$  per unit length of the beam [14]. Moreover, for the ELG beam incidence, the conservation of TAM of these beams follows directly from the conservation of TAM of each photon of which these beams are composed.

Above considerations pertain to the LG beams in their projected elegant version and of the circular polarization. In this case, the interface is acting, through the transmission matrices (32), within the complete set of such beams and produces pure eigenmodes with specified indices ( $p$  and  $l$ ) of the beam spatial structure in each one of the two (CR and CL) states of circular polarization. For beams of other spatial distribution of its complex amplitude and/or polarization, such as the standard LG beams of arbitrary polarization, the action of the interface may be understood as creating an appropriate superposition of pure projected ELG beams of circular polarization. In such cases, one has to consider mean values of TAM and OAM of these beams [19]. Still the conservation principles of TAM for a single photon (60) and for the total beam (61) remain valid.

The derivation of the conservation principle (55) and (56) for TAM of beams at the interface was possible due to the exact form of the transmission and reflection coefficients (32) and (33) or (12), (13), and (19). Both, the first-order and second-order transverse corrections [in  $k_Y$ , see Eq. (13)] to the standard Fresnel coefficients  $\eta_{t_p}$ ,  $t_s$ ,  $r_p$ , and  $r_s$  are necessary to obtain this result. The first-order corrections to the Fresnel coefficients, as well as these coefficients by themselves, are not sufficient to guarantee exactly the TAM conservation. Still, the TAM conservation (60) for a single photon was also approximately applied, instead of the field continuity relations, in the treatment of beams at a dielectric interface within a geometrical optics approach [36].

Note also that the ELG beams considered here possess cylindrical symmetry in the interface frame  $OXYZ$ . For incidence angles  $\theta^{(i)}$  different from zero, such beams are elliptic or astigmatic in their polarization, intensity, and phase distribution in their beam frames  $Oxyz$ . For instance, the polarization parameters  $\lambda_{(x,y)}^{(b)} = \pm i$  (11) of circularly polarized beams in the interface frame  $OXYZ$  reads for the same beams  $\lambda_{(x,y)}^{(b)} \cos \theta^{(b)} = \pm i \cos \theta^{(b)}$  in their beam frames  $Oxyz$  [5]. However, as orientation of their astigmatism is the same for their polarization, intensity, and phase, the OAM of the beams is originated only in the helical singularities of beam phase [37].

This is not so for beams of different orientation of their intensity and phase astigmatism. More general astigmatic beam modes may carry OAM not originated exclusively in the beam phase singularities [37]. Such beams also form complete sets of Gaussian solutions of the paraxial wave equation and may serve as another basis for treatment the problem of 3D beams impinging at the interface.

## VI. CONCLUSIONS

Beam-interface interactions have been described within a frame of the complete, biorthogonal sets of the projected

EHG beams of linear TM/TE uniform polarization and the projected ELG beams of circular CR/CL uniform polarization. It was shown that such beams are normal modes at the interface and, thus, in general, at any planar layered structure. The beam transverse spatial profile, phase, and polarization are interrelated through the XPC effect present at the interface. These relations differentiate normal and critical incidence of the beams and can be described by generalized Fresnel coefficients of transmission and reflection, specific to the incidence of beams of 3D structure and arbitrary polarization.

Rigorous analytical description of beam fields at the isotropic interface in terms of the projected EHG and ELG vector beam modes has been given. The interface redistributes incident beam energy between opposite polarization states of the beams and modifies spatial distribution of their intensity and phase. This process is quantitatively described through changes of indices of transverse spatial distribution of com-

plex beam fields or, for ELG beams of circular polarization, in terms of conservation of their TAM. In the latter case, changes of SAM are compensated by changes of OAM or vice versa. For incidence of beams of general phase and intensity distribution and general polarization, the interface discriminates the beam field in favor of EHG beam modes of linear polarization and of ELG beam modes of circular polarization. The process has been described by derivation of exact analytical expressions for spectral components of the beam field at the interface plane.

Characteristic features of the interface action may appear useful, for example, in beam sorting on the basis of SAM and OAM, provided that the efficiency of the XPC effect can be increased. It seems that application of the presented approach to the case of beams at layered structures, composed of anisotropic, photonic or metamaterials, may reveal such a possibility.

- 
- [1] L. Allen, M. W. Beijersbergen, R. J. C. Spreeuw, and J. P. Woerdman, *Phys. Rev. A* **45**, 8185 (1992).
- [2] P. Yeh, *Optical Waves in Layered Media* (Wiley, New York, 1976).
- [3] M. W. Beijersbergen, L. Allen, H. E. L. O. van der Veen, and J. P. Woerdman, *Opt. Commun.* **96**, 123 (1993).
- [4] L. Allen, J. Courtial, and M. J. Padgett, *Phys. Rev. E* **60**, 7497 (1999).
- [5] W. Nasalski, *Opt. Commun.* **197**, 217 (2001).
- [6] J. Lekner, *Theory of Reflection* (Kluwer, Dordrecht, 1978).
- [7] M. S. Soskin and M. V. Vasnetsov, *Prog. Opt.* **42**, 220 (2001).
- [8] J. P. Hugonin and R. Petit, *J. Opt. (Paris)* **8**, 73 (1977).
- [9] W. Nasalski, *J. Opt. Soc. Am. A* **13**, 172 (1996).
- [10] F. I. Baida, D. Van Labeke, and J.-M. Vigoureux, *J. Opt. Soc. Am. A* **17**, 858 (2000).
- [11] A. E. Siegman, *J. Opt. Soc. Am.* **63**, 1093 (1973).
- [12] T. Takenaka, M. Yokota, and O. Fukumitsu, *J. Opt. Soc. Am. A* **2**, 826 (1985).
- [13] S. Saghafi and C. J. R. Sheppard, *J. Mod. Opt.* **45**, 1999 (1998).
- [14] L. Allen, M. J. Padgett, and B. Babiker, *Prog. Opt.* **39**, 291 (1999).
- [15] A. T. O'Neil, I. Mac Vicar, L. Allen, and M. J. Padgett, *Phys. Rev. Lett.* **88**, 053601 (2002).
- [16] R. Zambrini and S. M. Barnett, *Phys. Rev. Lett.* **96**, 113901 (2006).
- [17] *The Physics of Quantum Information*, edited by D. Boumeester, A. Ekert, and A. Zeilinger (Springer, New York, 2000).
- [18] J. Leach, M. J. Padgett, S. M. Barnett, S. Franke-Arnold, and J. Courtial, *Phys. Rev. Lett.* **88**, 257901 (2002).
- [19] G. Molina-Terriza, J. P. Torres, and L. Torner, *Phys. Rev. Lett.* **88**, 013601 (2002).
- [20] A. Vaziri, G. Weihs, and A. Zeilinger, *Phys. Rev. Lett.* **89**, 240401 (2002).
- [21] J. Leach, J. Courtial, K. Skeldon, S. M. Barnett, S. Franke-Arnold, and M. J. Padgett, *Phys. Rev. Lett.* **92**, 013601 (2004).
- [22] M. Padgett, S. M. Barnett, and R. Loudon, *J. Mod. Opt.* **50**, 1555 (2003).
- [23] R. Loudon, S. M. Barnett, and C. Baxter, *Phys. Rev. A* **71**, 063802 (2005).
- [24] W. Nasalski, *J. Opt. A, Pure Appl. Opt.* **5**, 128 (2003).
- [25] W. Nasalski, *J. Tech. Phys.* **45**, 121 (2004).
- [26] M. Born and E. Wolf, *Principles of Optics*, 7th ed. (Cambridge University Press, Cambridge, England, 1999).
- [27] M. Lax, W. H. Louisell, and W. B. McKnight, *Phys. Rev. A* **11**, 1365 (1975).
- [28] W. Nasalski and Y. Pagani, *J. Opt. A, Pure Appl. Opt.* **8**, 21 (2006).
- [29] W. Nasalski and Y. Pagani, *Proc. SPIE* **6195**, 6195L-1 (2006).
- [30] J. Enderlein and F. Pampaloni, *J. Opt. Soc. Am. A* **21**, 1553 (2004).
- [31] J. B. Pendry, *Phys. Rev. Lett.* **85**, 3966 (2000).
- [32] M. Notomi, *Phys. Rev. B* **62**, 10696 (2000).
- [33] R. W. Ziolkowski and E. Heyman, *Phys. Rev. E* **64**, 056625 (2001).
- [34] A. E. Siegman, *Lasers* (University Science Books, Mill Valley, CA, 1986).
- [35] A. Kostenbauer, Y. Sun, and A. E. Siegman, *J. Opt. Soc. Am. A* **14**, 1780 (1997).
- [36] M. Onoda, S. Murakami, and N. Nagaosa, *Phys. Rev. Lett.* **93**, 083901 (2004).
- [37] J. Visser and G. Nienhuis, *Phys. Rev. A* **70**, 013809 (2004).